

# Non-degenerated sequential time-bin entanglement generation using periodically poled KTP waveguide<sup>1</sup>

Lijun Ma, Oliver Slattery, Tiejun Chang and Xiao Tang

*Information Technology Laboratory, National Institute of Standards and Technology,  
100 Bureau Drive, Gaithersburg, MD 20899  
[xiao.tang@nist.gov](mailto:xiao.tang@nist.gov)*

## ABSTRACT

We have experimentally implemented a non-degenerate sequential time-bin entangled photon-pair source using a periodically poled potassium titanyl phosphate (PPKTP) waveguide at a clock rate of 1 GHz. The wavelengths of the signal and idler are 895 and 1310 nm, which are suitable for local and long distance optical communications, respectively. A silicon avalanche photodiode (APD) is used to detect the photons at 895 nm while a periodically poled lithium niobate (PPLN) waveguide based up-conversion detector is used to detect the photons at 1310 nm. The measured entangled-photon-pair flux rate is 650 Hz and the visibility for two-photon interference fringe is 79.4 % without noise abstraction.

**Keywords:** quantum optics; nonlinear optics; parametric processes; waveguides.

## 1. INTRODUCTION

Entanglement is important for the realization of quantum communication, quantum teleportation and quantum computation. For a fiber-based quantum communications system, time-bin entanglement, or pulsed energy-time entanglement [1] is more suitable than polarization entanglement, since it is not sensitive to polarization changes in optical fibers. The original time-bin entanglement approach is realized using two consecutive laser pulses generated by an unbalanced interferometer to pump a nonlinear media. During the process, the two pulses have a certain probability to generate a photon pair by parametric down-conversion and implement the time-bin entangled photon pairs [1-4].

When a laser pulse train is used to pump the nonlinear media, and the condition  $T_c \gg \tau \gg \tau_p$  (where  $T_c$  is the coherence time of pump beam,  $\tau$  is the pulse interval,  $\tau_p$  is the pulse duration) is satisfied, a sequential time-bin entanglement can be generated [5-7]. The sequential time-bin entanglement scheme does not need an interferometer at the source side, and can achieve high-repetition rates which are more suitable for quantum communication. Several groups have successfully implemented high repetition rate sequential time-bin entanglement at the 1550 nm band using four-wave-mixing in dispersion shifted fiber [5] and periodically-poled LiNbO<sub>3</sub> (PPLN) waveguides [6,7].

In this paper, we report non-degenerate sequential time-bin entanglement generation using a periodically-poled potassium titanyl phosphate (PPKTP) waveguide at a repetition rate of 1 GHz. The signal and idler photons are 895 nm and 1310 nm, which are suitable for local and long distance optical networks, respectively. The 895 nm photon is resonant with the transition line of Cs atom, which potentially may be used for quantum memory. The conjugate

---

<sup>1</sup> The identification of any commercial product or trade name does not imply endorsement or recommendation by the National Institute of Standards and Technology.

wavelength is 1310 nm, a suitable wavelength for long distance quantum communication in coexistence with conventional 1550-nm signals in commercial optical networks.

## 2. SYSTEM CONFIGURATION

Figure 1 schematically shows the experimental setup. A continuous wave (CW) 1064-nm laser beam is emitted from a tunable laser (New Focus: TLB 6321). The emitted beam has a narrow line-width (300 KHz), which corresponds to a coherence time of 3.3  $\mu$ s. The coherence time satisfies the requirement to generate 1-GHz sequential time-bin entanglement. The CW laser is modulated into a 1-GHz pulse train with a FWHM of 330 ps by an amplitude modulator, and a pulse generator (Tektronix: DTG5274) provides the electrical pulse signal. In the mean time, another channel in the pulse generator provides a 1-GHz pulse train with a FWHM of 500 ps to the up-conversion detector for pulsed-pumping, and the time delay between the two channels is adjustable. The 1064-nm optical pulses are further amplified by a fiber amplifier (IPG: YAR-1K-LP) that can control the output power. A polarization controller (PC) is used to launch the proper polarization into the first PPKTP waveguide, which is used for the second harmonic generation (SHG) of 532-nm pump pulses. The pump pulses are then coupled into a 532-nm single-mode fiber, which removes the 1064-nm light and other noise from the fiber amplifier.

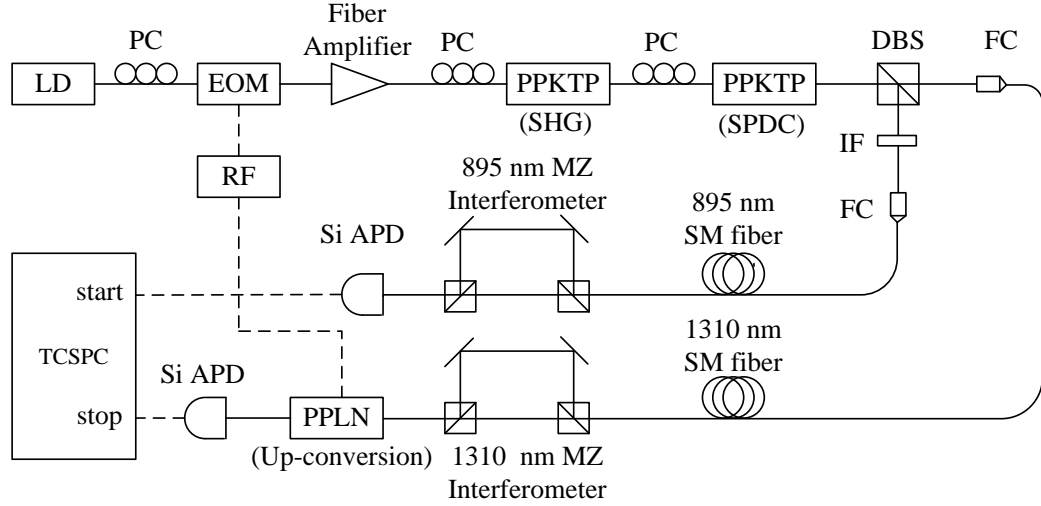


Fig. 1. Experimental setup. LD: 1064-nm CW laser Diode; EOM: Electric-optic Modulator; RF: RF pulse generator; PC: Polarization controller, PPKTP: Periodically-poled KTP waveguide; DBS: 895/1310 nm dichroic beam splitter; IF: Interference filter; FC: Fiber collimator; MZI: Mach-Zehnder interferometer; Si-APD: Silicon based avalanche photo diode; PPLN: Periodically-poled LiNbO<sub>3</sub> waveguide for frequency up-conversion; TCSPC: Time-correlated single photon counting module. Solid line: Optical path; Dash line: Electrical connection.

The second 2-cm long PPKTP waveguide is periodically poled to convert 532 nm to 1310 and 895 nm with type I phase matching and all vertically polarized. A series of time correlated photon pairs is generated in the waveguide by the spontaneous parametric down conversion (SPDC). By adjusting the pump power one can have on average of 1 pair of SPDC photons per  $N$  pump pulses. Under the condition  $N \gg 2$  and  $T_c \gg \tau \gg \tau_p$  (in our experiment, the coherence time of the pump laser  $T_c$  is 3.3  $\mu$ s, the pulse interval  $\tau$  is 1 ns, the pulse duration  $\tau_p$  is 330 ps), the quantum state of the photon pair is

$$|\Psi\rangle = \frac{1}{\sqrt{N}} \sum_{n=0}^{N-1} e^{in\phi_\tau} |n\tau\rangle_s |n\tau\rangle_i \quad (1)$$

where  $\phi_\tau$  is the phase difference between consecutive pump pulses, and s and i represents the signal (895 nm) and idler (1310 nm) photons. The signal and idler photons are separated using a dichroic beam splitter, and then coupled into 895 and 1310-nm single mode fibers, respectively. A bandpass filter is used to reduce the residual pump photons and other noise in the 895-nm photon path, while the noise in the 1310-nm path will be filtered by the up-conversion detector itself, which will be discussed in detail later.

To measure the two-photon-interference-fringe visibility, Franson type interferometers are needed [8]. We built two free-space unbalanced Mach-Zehnder interferometers (MZI) with 1 ns optical path difference. The phases of the interferometers are adjusted by a piezo nanopositioning stage. The insertion loss of the two interferometers is measured to be about 9 dB, which includes 3 dB intrinsic interferometer loss, fiber coupling loss, two path balance loss and other optical component losses. To avoid the influences from air turbulence and environmental vibration, the two interferometers are installed in a box and then mounted on an optical table with pneumatic vibration isolators. The visibility of the two MZI's is about 18 dB, and the visibility can be maintained for more than a half hour in our laboratory environment, which is long enough to finish our entanglement measurement. Temperature control is needed to achieve longer time stability.

A silicon-based avalanche photodiode (APD) (PerkinElmer: SPCM-AQR-14) is used to measure photons at 895 nm, and a PPLN waveguide-based up-conversion unit with another silicon-based APD [9] is used for photons at 1310 nm. We previously developed an up-conversion detector, and used it in a 1310-nm QKD system [9, 10]. Recently, we improved the up-conversion unit and increased its detection efficiency. The configuration of the up-conversion detector is shown in Fig. 2. Similar to our previous implementation, the 1550-nm light is modulated by sync signal and then amplified by an erbium-doped fiber amplifier (EDFA) (IPG: EAR-0.5K-C). Two 1550/1310 wavelength-division-multiplexer (WDM) couplers are used to remove the 1310-nm noise from the pump light, and another 1550/1310 WDM coupler is used to combine the 1310-nm photon under test and the 1550-nm pump light into one fiber and the combined signal and pump light is then coupled into a 5-cm long PPLN waveguide, where a single 1310-nm and one of the 1550-nm photons are converted in a sum-frequency-generation (SFG) process into 710 nm for the optimal detection. Two polarization controllers are used to align the polarization state of the signal and pump respectively. The main improvement in the new configuration is at the output side of waveguide. In our previous up-conversion detector, the output of PPLN waveguide is fiber coupled, which makes the detector compact. However, some noise is coupled into the same fiber, especially the SHG of the pump source at 775 nm, and therefore we needed to use several narrow bandpass filters to suppress the noise, which caused extra loss in the signal. In the new configuration, the output of the PPLN waveguide is coated with a 710-nm anti-reflection coating and the output is not coupled into a fiber, but rather left in free space. By using two dispersive prisms, the SFG photons at 710 nm are separated from both the pump beam at 1550 nm and its weak SHG noise at 775 nm, and then detected by a Si-APD. This configuration does not require fiber coupling, thus avoiding coupling loss, and only one bandpass filter is used to reduce noise. As a result, the total detection efficiency of the up-conversion detector for a certain wavelength near 1310 nm is increased to about 33%. With a pulsed pump at a wavelength longer than the quantum signal the up-conversion detector has a dark count rate as low as 2000 Hz. The detected signals are fed into a time-correlated single photon counting system (TCSPC) (PicoQuant: PicoHarp 300) for coincidence measurement.

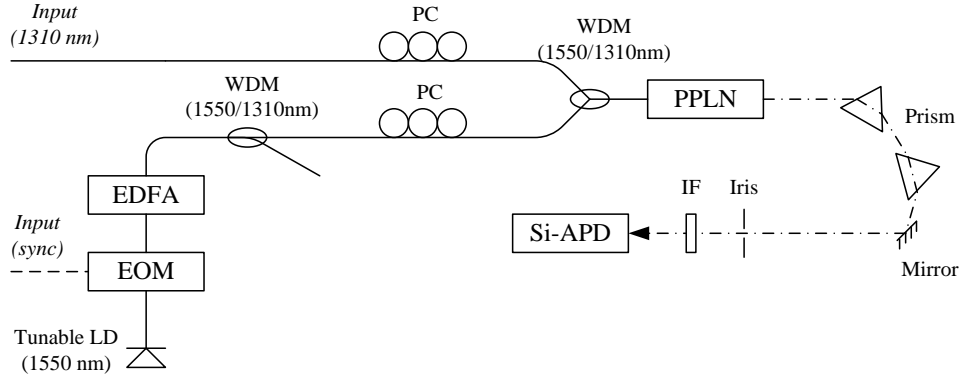


Fig. 2. Up-conversion detector. EOM: Electric-optic Modulator; EDFA: Erbium-doped fiber amplifier; WDM: Wavelength-division multiplexing coupler; PC: Polarization controller; PPLN: Periodically-poled LiNbO<sub>3</sub> waveguides; IF: Interference filter. Solid line: Optical fiber; Dash line: Free space optical transmission.

Fig.3 shows the spectrum of 1310-nm photons from the SPDC that is measured by an up-conversion spectrometer [11]. The spectral linewidth of the idler photons near 1310 nm is about 2 nm (FWHM). Since the spectral width is much wider than the acceptance bandwidth of the PPLN waveguide (0.2 nm), the quantum efficiency of the up-conversion detector is reduced to 3% when it is used to detect the 1310-nm photons generated from the SPDC. However, the narrow band pass property of the up-conversion detector provides an advantage. We do not need to use any additional narrow band pass filter in the 1310-nm optical path, since other photons at different wavelength do not satisfy the quasi-phase matching (QPM) condition for conversion and therefore cannot be detected.

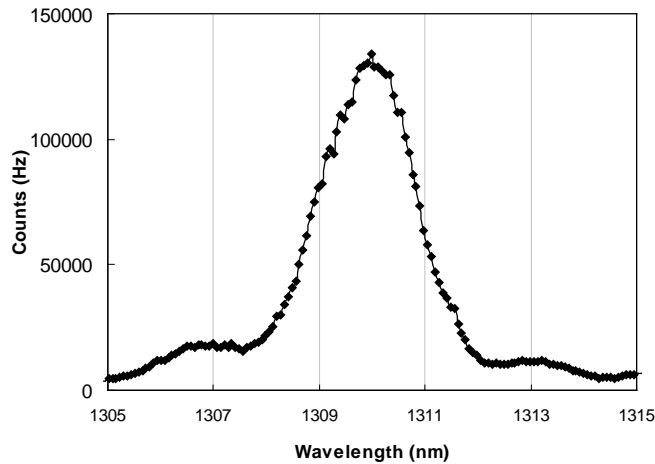


Fig. 3. A spectrum of the idler photons generated in the PPKTP waveguide near 1310 nm.

### 3. RESULTS AND DISCUSSION

In our experiment, amplified 1064-nm laser pulses (average power of 180 mW) are coupled into the SHG frequency doubler. The output laser pulses of average 0.25 mW at 532-nm are coupled into a 532-nm single mode fiber, and then guided into the second PPKTP for SPDC. The signal and idler photons are separated by the DBS, passed through their own MZI and then detected by a Si-APD and an up-conversion detector, respectively. Fig. 4 shows the histogram of coincidence photon pairs. The histogram shows three coincidence peaks, corresponding to the different optical paths in the interferometers that photon pairs pass through. The two side peaks show the coincidence that the two photons from

SPDC pass through different paths in the interferometers (long and short, or short and long, respectively). The two side peaks indicate which path the signal or idler photon passed through and there is no interference. The central peak records the coincidence counts where both photons pass through the same path, either both long paths, or both short paths. Because the two events (photons in the earlier time bin go through short and short paths, and those in the later time bin go through long and long paths) are indistinguishable and the phase difference between two adjacent time bins are the same as shown in Eq. (1), photon-pair interference occurs. The interference pattern can be estimated by the following equation [3]:

$$R_c = 1 - V \cos(\theta_s + \theta_i + \phi_\tau) \quad (2)$$

where  $R_c$  is the coincidence counting rate at the central peak;  $V$  is the visibility of the interference fringes;  $\theta_s$  and  $\theta_i$  are the phase difference between long and short paths in the interferometers for signal and idler respectively;  $\phi_\tau$  is the phase difference between consecutive pump pulses, which is the same as in Eq. (1). The coherence time of the pump is much longer than the time difference of the interference, so  $\phi_\tau$  is a constant. The interference pattern is determined by the relative phases of the two interferometers ( $\theta_s + \theta_i$ ).

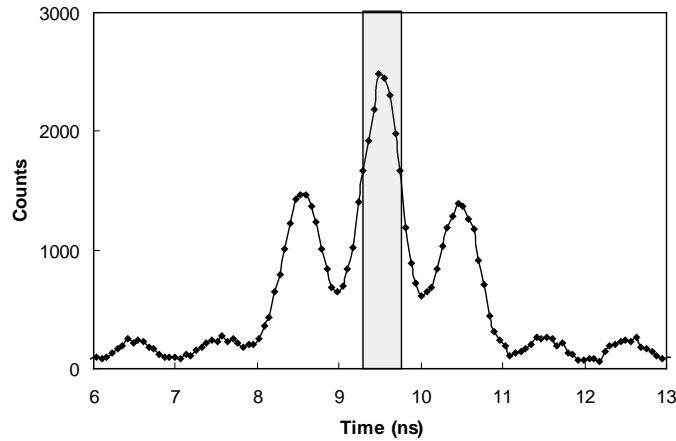


Fig. 4. Histogram of the coincidence counts of photon pairs after the two MZIs. The shaded area indicates the detection window (400ps)

From the histogram in Fig. 4, the timing jitter (FWHM) of the correlated photon pairs is 500 ps, which is mostly due to the timing jitter of two Si-APDs. Since the two side peaks have long time tails, they may leak into the time bin at the center and reduce the visibility, which is usually called inter-symbol interference. In order to minimize the influence of the side peak leakage, we assigned a detection time window around the center time slot. The worst visibility occurs when we chose a detection time window with a width as long as the clock period (1 ns), due to the inter-symbol interference. Using narrower detection time windows, we can improve the visibility. At the same time, however, the measured coincident photon number is somewhat reduced. Therefore, there is a compromise to choose the optimal time window between visibility and coincident photon number. In our experiment, we find a time window of around 400 ps is optimal for the measurement, which reduces the inter-symbol interference to less than 2% and reduces the coincidence counts by only 1.5 dB. The shaded area in Fig. 4 shows the detection time window.

In the Eq. (2), the interference fringe visibility,  $V$ , can be estimated by the following equation in our experiment [12]:

$$V = \frac{\mu\alpha_s\eta_s\alpha_i\eta_i}{\mu\alpha_s\eta_s\alpha_i\eta_i + 2\mu^2\alpha_s\eta_s\alpha_i\eta_i + 2\gamma\mu\alpha_s\eta_s\alpha_i\eta_i + \zeta\mu\alpha_s\eta_s\alpha_i\eta_i + 4\mu\alpha_s\eta_sD_it + 4\mu\alpha_i\eta_iD_it + 8D_iD_st^2} \quad (3)$$

Where  $\mu$  is the average photon pair number per pulse, which is about 0.08 in our case;  $\alpha_s$  and  $\alpha_i$  are the channel loss for signal and idler (16 dB for both channels);  $\eta_s$  and  $\eta_i$  are the quantum efficiencies of the single photon detectors for signal and idler (40% and 3%);  $\gamma$  is the inter-symbol interference caused by timing jitter (about 0.02);  $\zeta$  is imperfection of the interferometer (0.015 according to 18dB interferometer visibility);  $D_s$  and  $D_i$  are the dark count rate of the single photon detectors, which are 100 Hz and 2000Hz for signal and idler, respectively;  $t$  is the detection time window (400ps). By applying the above values into the equation, the calculated visibility of 81.4% is obtained.

In Eq. (3), the numerator is the coincidence due to entanglement. The second to forth terms in the denominator represent the multi-photon pair influence, inter-symbol interference and imperfection of the interferometer. These three components are the main contributions to the imperfection of the interference fringe visibility. To further increase the visibility, one needs to reduce the pump power and use high visibility interferometers and low timing jitter detectors. The last three items in Eq. (3) are the accidental coincidences between dark counts and photons from the SPDC and the accidental coincidence between dark counts of the two detectors. Due to the low dark count rate of the two detectors, the last three items do not contribute much to the degradation of visibility in our experiment. However, when the entangled photon source is used for transmission, the influence of the dark count-related noise components will be greater than other noise components and will become more significant in long distance distribution.

Piezo nano-positioning stages are used to set and vary the phase of both the signal interferometer and the idler interferometer. To determine the two-photon-interference-fringe visibility of the entangled photon pairs, we measured the photon coincidence through the interferometers, in which we fixed the phase for the signal interferometer (895 nm) and varied the phase for the idler interferometer (1310 nm). To demonstrate entanglement, we set two different fixed phases for the signal and got two interference patterns with the varied phase of the idler, as shown in Fig. 5. For each data point, we take measurement 6 times and then calculate the average value and their standard deviation used for the error bar. The average visibility of the two curves is 79.4% without subtraction of noise, which is close to our estimated value and is well beyond the 71% visibility for violation of the Bell inequality [13]. The measurement deviation is mainly caused by the temperature fluctuation of the interferometers.

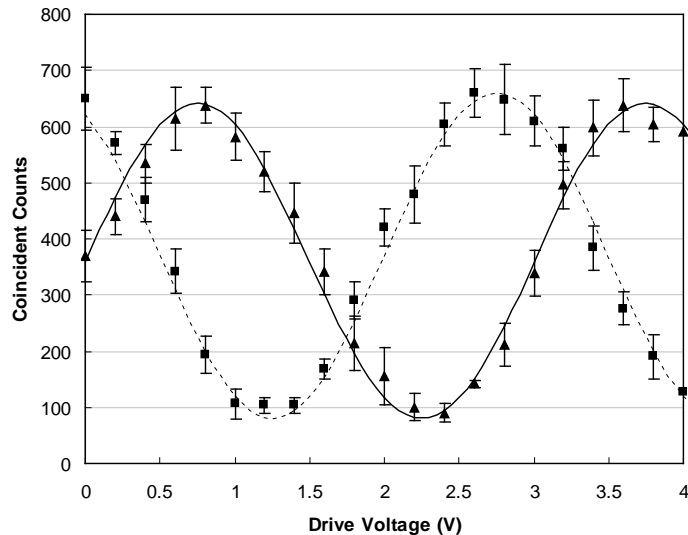


Fig. 5. Coincidence interference fringes measured in the experiments. Solid line/ triangle and dash line/square are the coincidence counts when the piezo drive voltages of 850-nm interferometer are 0 and 1 volt, respectively.

#### 4. CONCLUSION

In conclusion, we have implemented a sequential time-bin entanglement source using a PPKTP waveguide. The signal and idler photons are at 895 and 1310 nm, which are suitable for local and long distance optical networks, respectively. The entangled-photon-pair flux rate measured in the experiment is 650 Hz, which can be increased by reducing the loss of the transmission and in the interferometer and using high-efficiency single photon detectors. The two-photon-interference-fringe visibility of the entangled photon pairs is 79.4 % without abstraction of noise, which can be increased by reducing the pump power, using high visibility interferometers and low timing jitter detectors.

#### ACKNOWLEDGEMENT

Authors would like to thank Dr. Qiang Zhang from Edward L. Ginzton Laboratory, Stanford University for useful discussion. This research was supported by the NIST quantum information initiative.

#### REFERENCES

1. J. Brendel, N.Gisin, W. Tittel, and H. Zbinden, " Pulsed Energy-time entangled twin-photon source for quantum communication," *Physical Review Letters*, **82**, 2594-2596 (1999)
2. S. Tanzilli, W. Tittel, H. Riedmatten, H. Zbinden, P. Baldi, M Micheli, D. Ostrowsky, and N. Gisin, " PPLN waveguide for quantum communication," *European Physical Journal D*, **18**, 155-160 (2002)
3. I. Marcikic, H. Riedmatten, W. Tittel, V. Scarani, H. Zbinden, and N. Gisin, " Time-bin entangled qubits for quantum communication created by femtosecond pulses," *Physical Review A* **66**, 062308 (2002)
4. I. Marcikic, H. Ridmatten, W. Tittel, H. Zbinden, and N. Gisin, " Distribution of time-bin entangled qubits over 50 km of optical fiber," *Physical Review Letter*, **93**, 180502, (2004)
5. H. Takesue, and K. Inoue, " Generation of 1.5-um band entanglement using spontaneous fiber four-wave mixing and planar light-wave circuit interferometers," *Physical Review A* **72**, 041804 (2005)

6. T. Honjo, H. Takesue, H. Kamada, Y. Nishida, O. TAdanaga, M. Asobe and K. Inoue, “ Long-distance distribution of time-bin entangled photon pairs over 100 km using frequency up-conversion detectors,” *Optics Express*, **15**, 13957-13964 (2007)
7. Q. Zhang, C Langrock, H. Takesue, X. Xie, M. Fjer, and Y. Yamamoto, “ Generation of 10-GHz clock sequential time-bin entanglement” *Optics express*, **16** , 3293-3298 ( 2008)
8. J. Franson, “ Bell inequality for position and time,” *Physical Review Letter*, **62**, 2205 (1989)
9. H Xu, L. Ma, X. Tang, “Low noise PPLN-based single photon detector”, *SPIE Optics East 07* , Proc. SPIE. 6780, 67800U-1 (2007)
10. H. Xu, L. Ma, A. Mink, B. Hershman, and X. Tang “1310-nm quantum key distribution system with up-conversion pump wavelength at 1550 nm”, *Optics Express*, **15**, 7247~ 7260 (2007)
11. Q. Zhang, C. Langrock, M. Fejer, Y. Yamamoto, “ Waveguide-base single-pixel up-conversion infrared spectrometer,” *Optics Express*, **16**,19557~19561(2008)
12. Q. Zhang, H. Takesue, S. Nam, C. Langrock, X. Xie, B. Baek, M. Fejer, and Y. Yamamoto, “ Distribution of time-energy entanglement over 100 km fiber using superconduction single-photo detectors.”, *Optics Express*, **16**, 5776 (2008)
13. J. Clauser, M. Horne, A. Shimony, and R. Holt, “Proposed experiment to test local hidden-variable theories,” *Phys. Rev. Lett.* **23**, 880-884 (1969)